CHEMICAL ENGINEERING TRANSACTIONS
VOL. 101, 2023
A publication of AIDIC
The Italian Association of Chemical Engineering
Online at www.cetjournal.it
Guest Editors: Paolo Ciambelli, Luca Di Palma
Copyright © 2023, AIDIC Servizi S.r.l.
ISBN 979-12-81206-00-7; **ISSN** 2283-9216
DOI: 10.3303/CET23101020

Nanocellulose-based Aerogels for Dyes Removal

Annachiara Pirozzi[a,b,*], Esther Rincón[b], Eduardo Espinosa[b], Francesco Donsì[a], Luis Serrano[b]

[a]Department of Industrial Engineering, University of Salerno, via Giovanni Paolo II, 132, 84084 - Fisciano, Italy
[b]BioPrEn Group (RNM 940), Chemical Engineering Department, Instituto Químico para la Energía y el Medioambiente (IQUEMA), Faculty of Science, Universidad de Córdoba, 14014, Córdoba, Spain
apirozzi@unisa.it

Nanocellulose (NC) has recently emerged as of high interest in water purification because of its high surface area, aspect ratio, and versatile surface chemistry. In the present study, nanocellulose has been isolated from cellulose pulp, extracted from barley straw residues via a mechanical pulping treatment, through a combination of chemical and mechanical refining treatments. The obtained cellulose pulp and (ligno)cellulose nanofibrils (L)CNFs, in the form of papers and nanopapers, respectively, were characterized in terms of mechanical properties. Finally, (L)CNFs-based aerogels were developed, and adsorption tests at 25 °C using 0.1 g of aerogels in 50 mL of methylene blue (MB) dye solution at 10 mg/L were studied. The results revealed that CNF-based aerogels can be exploited as an effective eco-adsorbent for the removal of methylene blue dye and provide a new platform for dye removal.

1. Introduction

In recent years, cellulose has received increasing interest as a renewable raw material for producing biodegradable polymeric products and contributing to replacing fossil resources, considering their depletion, fluctuation in oil prices, and negative environmental impacts (Araújo et al., 2019). In the global scenario, the use of the vastly available by-products and residues along the whole food supply chain, also known as AFRs, is currently limited to livestock feed, providing a limited added value, or landfill or energy production by combustion, causing potential environmental issues (Collazo-Bigliardi et al., 2018). By virtue of their abundance and very low cost, AFRs possess a high chemical, material, and energy potential (Tuck et al., 2012). In industrial processing, vast amounts of AFRs are produced each year, which are mainly used as feed for livestock or agricultural supplements. The lignocellulosic matrix of plant cell walls, especially in agricultural residues, could also be used as a source of cellulose or nanocellulose. Cellulose, the most abundant organic compound on earth, is an unbranched polymer of D-glucose linked by β-1,4-glycosidic bonds. Compared with the α-1,4-glycosidic bonds, the β configuration allows cellulose to form very long and sturdy straight chains that could interact with each other via hydrogen bonds to form strong and degradation-resistant microfibrils (Poletto et al., 2014). Moreover, nanosized cellulosic (NC) materials possess several advantages deriving from their nanometric sizes, such as high tensile strength, stiffness, and surface functional groups (Pirozzi et al., 2021). The cellulosic materials having at least one dimension in the nanometric range, based on structure and particle diameters, can be extracted through a top-down process to obtain cellulose nanocrystals (CNCs) or cellulose nanofibers (CNFs); whereas bacterial cellulose (BC) is synthesized through a bottom-up approach (Rana et al., 2021). Owing to their excellent properties, NC recently gathered a relevant interest as an innovative platform for the production of aerogels with ultra-low density, high porosity, and large surface area, which can be exploited to remove organic dye from industrial wastewater by adsorption treatment in alternative to the commonly used polymeric and ceramic membranes, which have been shown to have less favourable effects on the environment. Therefore, this strategy is effective and eco-friendly because of its low cost and high efficiency, as well as because no harmful substances are generated. In this work, CNFs isolated from barley straw AFRs through a combination of chemical and mechanical treatments were used to produce aerogels and exploited to remove organic dye from industrial wastewater by adsorption treatment, using methylene blue as a model pollutant.

Paper Received: 16 January 2023; Revised: 3 April 2023; Accepted: 2 June 2023
Please cite this article as: Pirozzi A., Rincón E., Espinosa E., Donsì F., Serrano L., 2023, Nanocellulose-based Aerogels for Dyes Removal, Chemical Engineering Transactions, 101, 115-120 DOI:10.3303/CET23101020

2. Materials and Methods

2.1 Materials

The AFRs tested was barley straw (BS), provided by an industry in Córdoba (Spain). The barley straw, with 8.95 ± 0.23% of relative humidity, was stored in plastic bags until usage. Reagents used in this work consisted of sodium hydroxide (NaOH, ≥ 99%, Sigma Aldrich, St. Louis, MO, USA), hydrochloric acid (HCl, 37%, Sigma Aldrich, St. Louis, MO, USA), sodium chlorite ($NaClO_2$, ≥ 99%, Sigma Aldrich, St. Louis, MO, USA), sodium hypochlorite (NaClO, 10% w/v technical grade, PanReac, Barcelona, Spain), acetic acid (CH_3COOH, ACS reagent, Sigma Aldrich, St. Louis, MO, USA), sodium bromide (NaBr, Hoynewell, Muskegon, NC, USA), TEMPO, 2,2,6,6-tetramethyl-piperidin-1-oxyle ($C_9H_{18}NO$, 98%, Sigma Aldrich, St. Louis, MO, USA), ethanol (C_2H_5OH, Sigma Aldrich, St. Louis, MO, USA), sulphuric acid (H_2SO_4, 95-98%, labbox, Barcelona, Spain), methylene blue (labbox, Barcelona, Spain). All the reagents were used as received without further purification.

2.2 Cellulose pulp isolation process

Cellulose pulp was isolated from barley straw by alkaline hydrolysis in a 15 L batch reactor equipped with an external jacket and a motor to achieve the stirring of pulp suspension rotating the reaction vessel. The BS was subjected to a soda pulping process (NaOH at 7 wt% on dry basis, DM) for 150 min at 100 °C with a liquid/solid ratio of 10:1 (Eduardo Espinosa et al., 2019; Morcillo-Martín et al., 2022; Sánchez et al., 2016; Vargas et al., 2012). After the pulping process, the cellulosic pulp was washed, dispersed in a pulp disintegrator (Tendring Physical Testing Limited, UK) for 30 min at 1,200 rpm, and then fed to a refiner mechanical pulping Sprout-Bauer for facilitating the generation of shorter fibers. Finally, the pulp was filtered by sieving through a 0.14 mm mesh size and, after centrifugation to remove the excess water, dried at 60 °C for 24 h. Afterward, the obtained cellulose pulp was subjected to a bleaching process to eliminate the lignin content. Briefly, 0.3 $wt\%_{DM}$ of $NaClO_2$ was added in acidified conditions (2 vol% of acetic acid) to a 3 $wt\%_{DM}$ cellulose pulp suspension at 80 °C for 1 h. This treatment was repeated three times to achieve the final bleached and purified cellulose fibers (BS-B); unbleached pulp (BS-UB) was, instead, characterized by a residual lignin content in the final product.

2.3 Cellulose pulp characterization

Fourier-transform infrared (FT-IR) spectroscopy was used to identify the main functional groups and chemical structure of BS-UB and BS-B, with an FT-IR Spectrum Two series spectrophotometer (PerkinElmer, Waltham, Massachusetts, United States) at ambient conditions. The infrared spectra were collected in transmittance mode from an accumulation of 40 scans over the wavenumber regions of 4000 - 400 cm^{-1} at a resolution of 4 cm^{-1}. The resulting spectra were smoothed with a five-point under adaptive-smoothing function to remove the eventual noises, and then baseline modification was applied.

2.4 Nanocellulose isolation

To obtain (ligno)cellulose nanofibers ((L)CNFs), two different pre-treatments were used on BS-UB and BS-B: (i) chemical process by TEMPO-mediated oxidation and (ii) mechanical beating by mechanical refining. The TEMPO-mediated oxidation pre-treatment was carried out by suspending cellulose fibers at a final concentration of 1 wt_{DM} in distilled water containing TEMPO catalyst (0.016 $wt\%_{DM}$) and sodium bromide (0.1 $wt\%_{DM}$). The TEMPO-mediated oxidation was started by adding a specific amount of NaClO solution to obtain an oxidative power of 5 $mmol/g_{DM}$ with continuous stirring at 25 °C. The pH of the suspension was maintained at 10 by adding NaOH solution (0.5 M) until no NaOH consumption was observed. After about 2 h of reaction time, 100 mL of ethanol was added to stop the oxidation reaction, and the oxidized fibers were filtered and washed several times with distilled water (Besbes et al., 2011). The mechanical pre-treatment was carried out by refining the cellulose fibers suspension (10 $wt\%_{DM}$) at 20,000 rpm in a PFI beater (Mill PFI type, Metrotec, Kirchheim, Germany) to reach a Schopper–Riegler Degree (ºSR) of 90, according to ISO 5264-2:2002. A 1 $wt\%_{DM}$ suspension of pre-treated fibers was subjected to a nanofibrillation process in a high-pressure homogenizer (PandaPlus 2000, GEA Niro, Düsseldorf, Germany) following 4 passes at 300 bars, 3 passes at 600 bars, and 3 passes at 900 bars (Eduardo Espinosa et al., 2017). Nanocellulose obtained from unbleached cellulose pulp (BS-UB) were designed as LCNF (cellulose nanofibers with residual lignin content in the final product); meanwhile, nanocellulose obtained from bleached cellulose pulp (BS-B) were designed as CNF. Moreover, LCNF and CNF were obtained either by TEMPO-mediated oxidation pre-treatment (designed as LCNF-TO and CNF-TO, respectively) or PFI beater mechanical pre-treatment (designed as LCNF-Mec and CNF-Mec, respectively).

2.5 Cellulose and nanocellulose papers preparation and characterization

The cellulosic pulp (BS-UB and BS-B) and nanocellulose (LCNF-TO, CNF-TO, LCNF-Mec, and CNF-Mec) were dispersed in a pulp disintegrator at a final concentration of 0.5 $wt\%_{DM}$. The suspension was filtered under vacuum at -600 mbar until the removal of supernatant water in a sheet former (Rapid Kothen, ISO 5269-2).

Afterward, sheets were dried at 85 °C between two nylon sieves to prevent adherence and two cardboards until the papers and nanopapers were completely dried. All papers were stored for 48 h in a conditioned room at 24 °C and 50% RH before characterization.
The tensile properties were measured with Lloyd LF Plus Tensile Test Machine (Lloyd Instruments Ltd, Bognor Regis, United Kindom) equipped with a 1 kN load cell, following the standard NF Q03-004. The mechanical properties of the papers were evaluated by tensile tests, performed on rectangular samples (10 cm length and 15 mm width) with an initial gauge length of 10 cm and a crosshead speed of 10 mm/min. The thickness was measured using a high accuracy Digital Micrometer (Mitutoyo Europe GmbH, Elgoibar, Spain).

2.6 (L)CNFs-based aerogels

(L)CNF at 0.5 $wt\%_{DM}$ were prepared by diluting the samples with distilled water and homogenizing at 20,000 rpm for 5 min with an Ultraturrax T18 (IKA-Werke GmbH & Co. KG, Staufen, Germany). Each suspension was frozen prior to freeze-drying under 0.5 mBar for 72 h (Lyoquest -85 lyophilizer, Telstar, Terrassa, Spain).

2.7 Methylene blue adsorption

Adsorption experiments were performed by immersing the aerogel samples in 50 mL methylene blue (MB) dye aqueous solution at 10 mg/L. The concentration of the dye solution during 24 h of adsorption was analyzed by UV-vis spectrophotometer (Lambda 25, Perkin Elmer Inc, Waltham, USA), using a calibration curve, obtained from the linear fitting of the measured absorbance (A664 nm) as a function of methylene blue concentration (ranging from 0 to 10 mg/L).

2.9 Statistical analysis

Analyses were performed in triplicate unless differently specified and the results were reported as means ± standard deviations. Differences among mean values were analyzed by one-way variance (ANOVA), performed with SPSS 20 (SPSS IBM., Chicago, USA) statistical package, and Tukey test was performed to determine statistically significant differences ($p < 0.05$).

3. Results and discussions

3.1 Cellulose pulp characterization

FT-IR spectra of extracted celluloses (Figure 1) were measured to evaluate the structural changes that occurred during the applied treatments (Pirozzi et al., 2022) and investigate the effect of bleaching conditions on the quality of the celluloses.

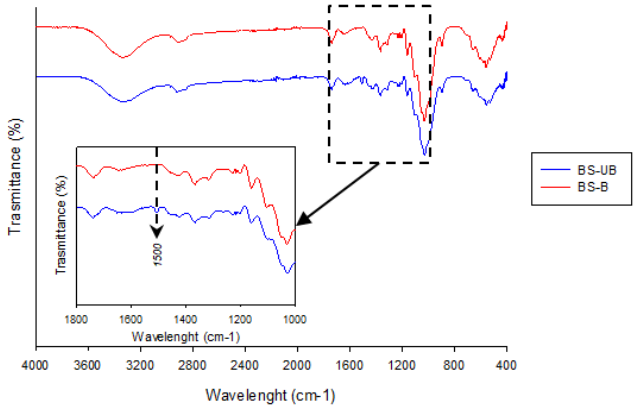

Figure 1: FT-IR spectra of unbleached (BS-UB) and bleached (BS-B) cellulose pulp

All spectra showed some signature characteristic bands of celluloses, including absorption peaks at 3300 and 2902 cm^{-1} because of the presence of H–bounded OH group stretching and C-H stretching vibration groups (Ling et al., 2021), respectively. In addition, the peak at 1028 cm^{-1} belongs to the C-O-C pyranose ring stretching vibration (Kubovský et al., 2020; Ling et al., 2021) and 897 cm^{-1} at C-O-C stretching at the β-(1-4)glycosidic linkages between sugar units (Zhuang et al., 2020). The next peak detected in the spectra of unbleached cellulose pulp is around 1500 cm^{-1} (C=C aromatic skeletal vibrations stretching of the benzene ring), corresponding to the aromatic ring of lignin (Kubovský et al., 2020). The absence of this band from the spectrum of bleached cellulose pulp attested to the efficiency of lignin removal during the bleaching process.

Thus, the accessibility of functional groups is facilitated, making the fibers more amenable to functionalization by chemical or physical pre-treatments and favoring their subsequent defibrillation.

3.2 Papers and nanopapers characterization

Papers from BS-UB and BS-B cellulose pulp (data not shown) exhibited a homogenous surface characterized by large and macroscopically heterogeneous spots and visible white agglomerates. In contrast, nanopapers prepared from CNFs suspension generally showed a semi-transparent and smooth appearance without any holes. Mechanical properties and porosity of the derived papers and nanopapers using extracted cellulose pulp and isolated cellulose nanofibers are reported in Table 1. Nanopapers containing NCs isolated through mechanical treatments exhibited the highest tensile strength and load at break among all the papers. Due to the number of links among fibers, the type of links, and the intrinsic resistance of the fiber, LCNF-Mec and CNF-Mec demonstrated to possess a better adhesion between the cellulose fibers, resulting in superior mechanical strength of paper sheets. More specifically, nanopaper from LCNF-Mec and CNF-Mec suspensions exhibited the highest tensile strength values (28.62 ± 2.13 and 28.92 ± 3.50 MPa, respectively), which was significantly ($p < 0.05$) higher than for CNF-TO (65 and 68% increase, respectively). A lower tensile strength caused a reduction in flexibility. Furthermore, the crosslinking among mechanical pre-treated complexed NC networks enabled the enhancement of the strain at break of the nanopaper, with an increase in comparison with CNF-TO of 105 and 207% for LCNF-Mec and CNF-Mec, respectively. This improvement was likely due to the enhanced interactions of the NCs constituents of the nanopaper, promoted by the electrostatic forces (Zhang et al., 2021).

Table 1: Mechanical properties from the elongation analysis of papers and nanopapers

	Tensile strength (MPa)	Load at break (N)	Strain at Break (%)
BS-UB	3.98 ± 0.91^{a}	12.06 ± 1.87^{a}	1.10 ± 0.20^{a}
BS-B	11.44 ± 1.27^{b}	25.85 ± 0.40^{b}	1.72 ± 0.38^{b}
LCNF-TO	7.63 ± 1.04^{ab}	9.49 ± 0.98^{a}	1.02 ± 0.06^{a}
CNF-TO	17.33 ± 0.15^{c}	9.02 ± 0.35^{a}	0.86 ± 0.28^{a}
LCNF-Mec	28.62 ± 2.13^{d}	31.48 ± 2.28^{c}	1.76 ± 0.17^{b}
CNF-Mec	28.92 ± 3.50^{d}	28.99 ± 0.73^{c}	1.79 ± 0.19^{b}

Different letters denote significant differences ($p < 0.05$) among the different samples within each column (n = 3)

3.3 Adsorption capacity of (L)CNF aerogels

The methylene blue (MB) concentration was evaluated during 24 h of adsorption test using the calibration curve (Figure 2) prepared by reading the absorbance of the MB, at a wavelength of 664 nm, when mixed with serial dilutions starting from the stock solution of 10 mg/L. The linear correlation between the UV-VIS absorbance and the MB concentration, expressed through Equation 1, was very high (R^2= 0.999).

$$Abs|_{664\,nm} = 0.207 \cdot MB_{concentration} \quad (1)$$

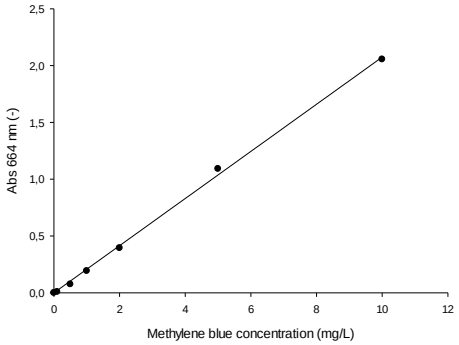

Figure 2: Calibration curve for UV-Vis absorbance of methylene blue

Moreover, from the calibration curve, according to Lambert Beer's law, it was possible to determine the molar absorptivity of MB at 664 nm, which is about ε = A/(C·L) = 0.174 L/(mg·cm).
The adsorption capacities of (L)CNFs-based aerogels for MB cationic dye are shown in Table 2. These findings show that the adsorption capacities for MB increased with increasing contact time and that the adsorption processes reached equilibrium within about 120 min. Moreover, a rapid increase in the capacities for the dyes occurred during the first 30 min. The fast adsorption at the initial stage might be due to the availability of the

uncovered surface area and the remaining active sites on the adsorbent. Therefore, all samples exhibited a very high adsorption capacity for the dye, allowing them to obtain a final MB solution concentration ranging between 0.72 and 4.24 mg/L. In addition, the adsorption capacity of CNF-TO aerogel was larger than for CNF-Mec aerogel, which indicated that TEMPO-oxidation treatment allowed to obtain cellulose nanofibers with higher specific surface area and therefore higher affinity and interaction of carboxyl groups with methylene blue. Moreover, it is likely that the residual lignin content in LCNF-based aerogels efficiently interacted with the cationic organic dye: together with the high adsorption capacity of cellulose nanofibers, demonstrated a synergistic effect in their use as materials with a high adsorption capacity.

Table 2: Concentration variation of MB solution during 24 h of adsorption test with (L)CNFs-based aerogels

Time (min)	LCNF-TO	CNF-TO	LCNF-Mec	CNF-Mec
0	10.29 ± 0.46	10.29 ± 0.46	9.99 ± 0.42	9.99 ± 0.42
5	2.68 ± 0.09	7.78 ± 0.06	9.74 ± 0.11	5.56 ± 0.77
30	1.12 ± 0.04	3.48 ± 0.75	8.37 ± 1.02	5.43 ± 0.77
60	1.03 ± 0.02	1.66 ± 0.69	7.77 ± 0.83	5.32 ± 0.79
120	0.91 ± 0.02	0.78 ± 0.24	6.00 ± 0.01	4.82 ± 0.76
180	0.92 ± 0.08	0.62 ± 0.07	4.68 ± 0.04	4.76 ± 0.72
240	0.96 ± 0.02	0.69 ± 0.11	3.80 ± 0.24	4.47 ± 0.93
1380	1.09 ± 0.04	0.70 ± 0.01	0.89 ± 0.06	4.30 ± 0.72
1440	1.27 ± 0.10	0.72 ± 0.07	0.83 ± 0.12	4.24 ± 0.74

Visual observations (Figure 3) clearly show how the MB solution became fainter after the adsorption of the dye with the aerogels.

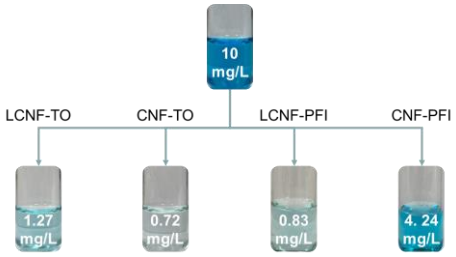

Figure 3: Digital photos of MB solution before and after adsorption test with (L)CNFs-based aerogels

These results show that nanocellulose from barley straw is a promising material for wastewater treatment due to the electrostatic interactions and the availability of a large number of -OH groups on the aerogels surface able to adsorb the cationic dyes within a short time, as mentioned in many previous literature studies (Wang et al., 2021; Zhu et al. 2021). In this study, this is the first time aerogels have been prepared with CNFs extracted from the barley straw, which is a by-products and exhibited a significant removal of MB through the blue color of MB fading with contact time without the usage of reinforcement materials, such as graphene oxide.

4. Conclusions

The usage of barley straw, which is agricultural by-products and actually waste materials, for nanocellulose isolation provides a way to produce a new generation and highly versatile nanomaterial resolving at the same time the environmental issues. NC possesses a wide range of favourable properties, such as high mechanical strength, which make it a suitable and promising low-cost material for use as a membrane material in industrial applications such as in wastewater treatment systems. The results showed that the stable and porous three-dimensional network structure of (L)CNFs-based aerogels have a high adsorption capacity for MB cationic dye, giving it an advantage over other engineering materials used in water treatment systems, for example polymeric materials. Further, more studies need to be done in the frame of adsorption to evaluate the adsorption capacity of these adsorbent materials reuse for subsequent cycles.

Acknowledgments

This research was funded by the Italian Ministry of University (MUR) call PRIN 2017 with the project 2017LEPH3M “PANACEA: A technology PlAtform for the sustainable recovery and advanced use of NAnostructured CEllulose from Agro-food residues”.

References

Araújo D.J.C., Machado A.V., Vilarinho M.C.L.G., 2019, Availability and Suitability of Agroindustrial Residues as Feedstock for Cellulose-Based Materials: Brazil Case Study, Waste and Biomass Valorization, 10, 2863-2878.

Besbes I., Alila S., Boufi S., 2011, Nanofibrillated cellulose from TEMPO-oxidized eucalyptus fibres: Effect of the carboxyl content, Carbohydrate Polymers, 84, 975-983.

Collazo-Bigliardi S., Ortega-Toro R., Chiralt Boix A., 2018, Isolation and characterisation of microcrystalline cellulose and cellulose nanocrystals from coffee husk and comparative study with rice husk. Carbohydrate Polymers, 191, 205-215.

Espinosa E., Rol F., Bras J., Rodríguez A., 2019, Production of lignocellulose nanofibers from wheat straw by different fibrillation methods. Comparison of its viability in cardboard recycling process, Journal of Cleaner Production, 239, 118083.

Espinosa E., Sánchez R., González Z., Domínguez-Robles J., Ferrari B., Rodríguez A., 2017, Rapidly growing vegetables as new sources for lignocellulose nanofibre isolation: Physicochemical, thermal and rheological characterisation, Carbohydrate Polymers, 175, 27-37.

Kubovský I., Kačíková D., Kačík F., 2020, Structural Changes of Oak Wood Main Components Caused by Thermal Modification, Polymers, 12, 485.

Ling Z., Tang W., Su Y., Shao L., Wang P., Ren Y., Huang C., 2021, Promoting enzymatic hydrolysis of aggregated bamboo crystalline cellulose by fast microwave-assisted dicarboxylic acid deep eutectic solvents pretreatments, Bioresource Technology, 333, 125122.

Morcillo-Martín R., Espinosa E., Rabasco-Vílchez L., Sanchez L. M., de Haro J., Rodríguez A., 2022, Cellulose Nanofiber-Based Aerogels from Wheat Straw: Influence of Surface Load and Lignin Content on Their Properties and Dye Removal Capacity, Biomolecule, 12, 232.

Pirozzi A., Capuano R., Avolio R., Gentile G., Ferrari G., Donsì F., 2021, O/W pickering emulsions stabilized with cellulose nanofibrils produced through different mechanical treatments, Foods, 10, 1886.

Pirozzi A., Ferrari G., & Donsì F., 2022, Cellulose Isolation from Tomato Pomace Pretreated by High-Pressure Homogenization, Foods, 11, 266.

Poletto M., Ornaghi Júnior H. L., Zattera A. J., 2014, Native cellulose: Structure, characterization and thermal properties, Materials, 7, 6105-6119

Rana A. K., Frollini E., Thakur V. K., 2021, Cellulose nanocrystals: Pretreatments, preparation strategies, and surface functionalization, International Journal of Biological Macromolecules, 182, 1554-1581.

Sánchez R., Espinosa E., Domínguez-Robles J., Loaiza J. M., Rodríguez A., 2016, Isolation and characterization of lignocellulose nanofibers from different wheat straw pulps, International Journal of Biological Macromolecules, 92, 1025-1033.

Tuck C. O., Pérez E., Horváth I. T., Sheldon R. A., Poliakoff M., 2012, Valorization of biomass: Deriving more value from waste, Science, 337, 695-699

Vargas F., González Z., Sánchez R., Jiménez L., Rodríguez A., 2012, Cellulosic pulps of cereal straws as raw material for the manufacture of ecological packaging, BioResources., 7, 4161-4170.

Zhang K., Ismail M. Y., Liimatainen H., 2021, Water-resistant nanopaper with tunable water barrier and mechanical properties from assembled complexes of oppositely charged cellulosic nanomaterials, Food Hydrocolloids, 120, 106983.

Zhuang J., Li M., Pu Y., Ragauskas A.J., Yoo C.G., 2020, Observation of Potential Contaminants in Processed Biomass Using Fourier Transform Infrared Spectroscopy, Applied Sciences, 10, 4345.

Wang, Z.; Song, L.; Wang, Y.; Zhang, X.-F.; Yao, J., 2021, Construction of a Hybrid Graphene Oxide/Nanofibrillated Cellulose Aerogel Used for the Efficient Removal of Methylene Blue and Tetracycline, J. Phys. Chem. Solids, 150, 109839.

Zhu, W.; Jiang, X.; Jiang, K.; Liu, F.; You, F.; Yao, C., 2021, Fabrication of Reusable Carboxymethyl Cellulose/Graphene Oxide Composite Aerogel with Large Surface Area for Adsorption of Methylene Blue, Nanomaterials, 11, 1609.